Despeckling vs Averaging of retinal UHROCT tomograms: advantages and limitations

Justin A. Eichel[1], Donghyun D. Lee[2], Alexander Wong[1],
Paul W. Fieguth[1], David A. Clausi[1], and Kostadinka K. Bizheva[2]

[1]Systems Design Engineering, University of Waterloo, Waterloo, Ontario, Canada
[2]Department of Physics and Astronomy, University of Waterloo, Waterloo, Ontario, Canada

ABSTRACT

Imaging time can be reduced using despeckled tomograms, which have similar image metrics to those obtained by averaging several low speed tomograms or many high speed tomograms. Quantitative analysis was used to compare the performance of two speckle denoising approaches, algorithmic despeckling and frame averaging, as applied to retinal OCT images. Human retinal tomograms were acquired from healthy subjects with a research grade $1060nm$ spectral domain UHROCT system with $5\mu m$ axial resolution in the retina. Single cross-sectional retinal tomograms were processed with a novel speckle denoising algorithm and compared with frame averaged retinal images acquired at the same location. Image quality metrics such as the image SNR and contrast-to-noise ratio (CNR) were evaluated for both cases.

Keywords: Optical coherence tomography, image processing, speckle, biomedical optics, medical imaging

1. INTRODUCTION

Optical coherence tomography (OCT) is a minimally invasive imaging technique, based on low-coherence interferometry, that utilizes the spatial and temporal coherence properties of optical waves backscattered from biological tissue. Since OCT is based on detection of partially coherent light, speckle noise is an inherent component of any OCT tomogram.

The presence of speckle noise results in granular appearance of the image, which in turn can obscure small or low reflectivity features, thus degrading the image quality. Furthermore, it can impede or limit the performance of image segmentation and pattern recognition algorithms that are used to extract, analyze, and recognize diagnostically relevant features.

Both algorithmic (i.e. filtering techniques or anisotropic diffusion) and hardware (i.e. frequency or angular compounding) approaches have been used the past to reduce speckle noise in OCT images. The first approach requires processing time that is considerably longer than the acquisition time of a single cross-sectional OCT tomogram therefore, it is currently unsuitable for real time viewing of processed OCT images. The second approach adds to the complexity of the OCT system design and image acquisition procedure.

A simpler approach to speckle noise reduction that can be applied in real time is frame averaging, which comprised acquisition of multiple cross-sectional OCT images from the same location in the imaged object and subsequent registration and weighted summation of the frames. Although this approach has proven useful in improving the overall image quality of OCT tomograms as viewed in real time, it has a few significant drawbacks: a) the acquisition of N frames at the same sample location increased the overall image acquisition time by a factor of N; and b) in the presence of fast sample motion, the averaging of the multiple frames needs to be

Further author information: (Send correspondence to J.A.E)
J.A.E.: E-mail: jaeichel@engmail.uwaterloo.ca
D.D.L.: E-mail: d47lee@uwaterloo.ca
A.W.: E-mail: a28wong@engmail.uwaterloo.ca
P.W.F.: E-mail: pfieguth@uwaterloo.ca, Telephone: +1 519 888 4567 x 33599
D.A.C.: E-mail: dclausi@engmail.uwaterloo.ca, Telephone: +1 519 888 4567 x 32604
K.K.B.: E-mail: kbizheva@sciborg.uwaterloo.ca, Telephone: +1 519 888 4567 x 35665

Optical Coherence Tomography and Coherence Domain Optical Methods in Biomedicine XV, edited by James G. Fujimoto, Joseph A. Izatt, Valery V. Tuchin, Proc. of SPIE Vol. 7889, 78893C · © 2011 SPIE · CCC code: 1605-7422/11/$18
doi: 10.1117/12.875867

Downloaded from SPIE Digital Library on 08 Jul 2011 to 129.97.72.149. Terms of Use: http://spiedl.org/terms

preceded by image registration, which is time consuming and its precision is strongly dependent on the type and magnitude of the sample motion. Imprecise registration of a limited number of images can result in blur of the frame-averaged tomogram, which will reduce the visibility of fine morphological features in the image.

The earliest speckle reduction methods employ linear filtering strategies,[4–6] which are effective at suppressing speckle but also significantly degrades important image detail. Subsequent methods employed more advanced nonlinear strategies such as adaptive median filtering,[7] maximum a posteriori (MAP) estimation,[8] and anisotropic diffusion.[9,10] These methods provide good speckle reduction capabilities and better detail preservation than the earlier methods, but still suffer from degradation in fine image detail. More recently, multiscale methods based on manipulating wavelet coefficients[11,12] have proven to provide more effective speckle reduction as well as detail preservation by considering details at different scales.

Here we present a quantitative comparison between image despeckling and frame averaging approaches to processing retinal OCT tomograms. The results from this study could serve as a guide to the conditions under which one or the other image processing approach would be optimal for retinal OCT tomograms.

2. METHODS

All human retina tomograms used in this project were acquired with a high speed $1060nm$ ultra-high resolution optical coherence tomography (UHROCT) system,[1] based on a compact fiber optic Michelson interferometer, connected to a superluminescent diode, SLD (Superlum Ltd., $\lambda_c = 1020nm$, $\Delta\lambda = 110nm$). The UHROCT system provided $5\mu m$ axial and $10\mu m$ lateral resolution in retinal tissue and $95dB$ SNR at 92,000 A-scans/s image acquisition rate, for $1.5mW$ power of the imaging beam at the cornea. Up to 30 cross-sectional 2D images were acquired from the same location in the retina, in-vivo from the fovea and optic nerve head of healthy human subjects. The imaging procedure was approved by the University of Waterloo Human Ethics Committee.

Composite images are created by averaging each set of tomograms that are obtained from imaging the same retinal location. Each tomogram in the set was manually aligned by displaying an alternating pattern of the candidate tomogram against a reference tomogram; the two tomograms would alternatively flicker in a display. A user can adjust the translation offset in the x and y direction of the imaging plane and could rotate the candidate tomogram about a desired pivot point to a specified angle. The user can manipulate the parameters until no significant motion, due to flickering, is observed. At this time, the user indicates that the candidate tomogram has been aligned with a reference tomogram and continues to align the remaining images in the set. While automated registration algorithms exist, this manual method was selected because it allows the expert user to accurately align the images without the biases associated with automated algorithms. Existing automated registration algorithms may be inappropriately applied to retinal alignment if their underlying assumptions are not clearly understood. This study assumes that an accurate registration is somehow obtained. Composite images are generated using groups of 2, 5, 10, 15, 20, 25 and 30 tomograms obtained from imaging the same retinal location.

The composite images are then compared to the results of despeckling a single tomogram using a novel algorithm.[2] In that algorithm, the image is projected into the logarithmic space, and the speckle reduction problem is formulated as a general Bayesian least squares problem. Based on this formulation, an estimate of the speckle-free image is computed based on a conditional posterior sampling strategy.

The original, composite images, and the despeckled images were then compared using image quality metrics such as signal-to-noise ratio (SNR) and contrast-to-noise ratio (CNR) in order to determine how well despeckling compares to averaging tomograms. The results, shown in the following section, indicate how despeckling can improve image quality while imaging at high speeds.

3. RESULTS AND DISCUSSION

Tomograms for this study represent 13 datasets collected from 4 healthy subjects at imaging speeds of 47,000 and 92,000 A-scans/s. For each dataset, the tomograms were manually registered using the process described in the previous section; the composite tomograms could be constructed by averaging two or more of the registered images. In addition, the despeckling algorithm[2] with $\sigma = 19$, $\sigma = 26$, and $\sigma = 32$ was applied to each single tomogram.

Downloaded from SPIE Digital Library on 08 Jul 2011 to 129.97.72.149. Terms of Use: http://spiedl.org/terms

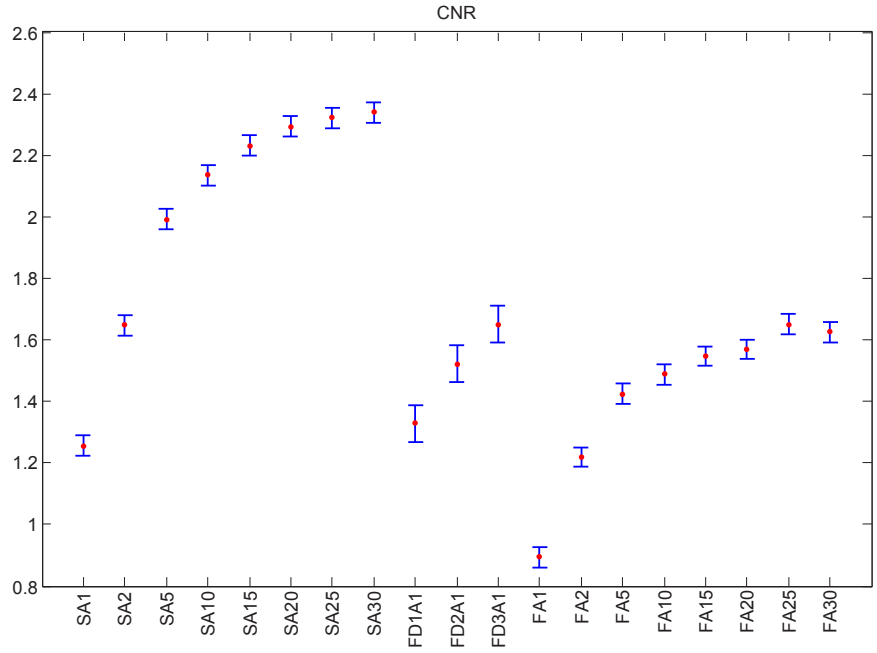

(a)

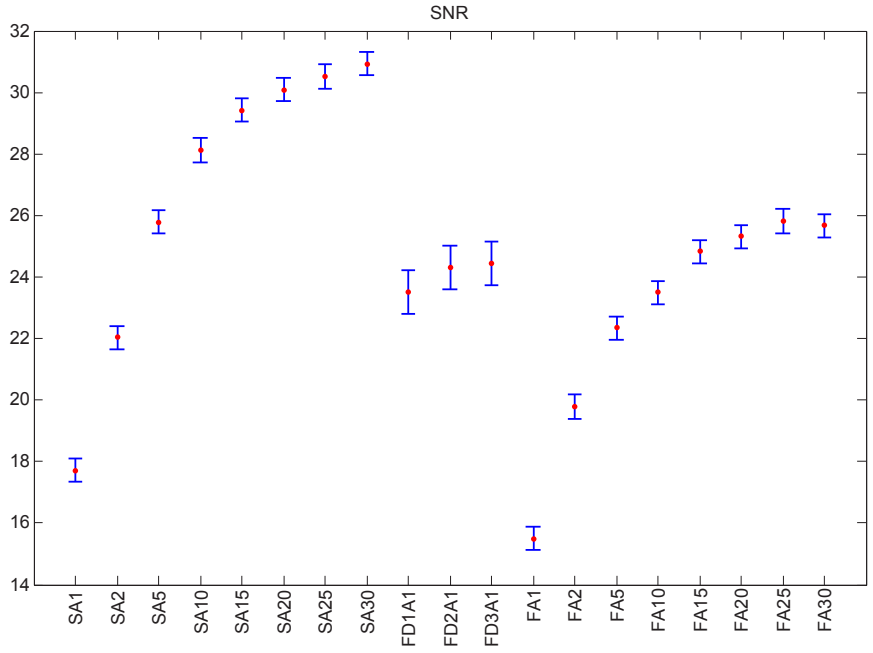

(b)

Figure 1. (a) CNR results. (b) SNR results. 19 statistical groups are compared using anova to determine which groups have statistically different means. The first 8 groups, SA1, SA2, ..., SA30, are composites containing 1, 2, ..., 30 images at 47,000 A-scans/s. The following 3 groups, FD1A1, FD2A1, and FD3A1, are despeckled 92,000 A-scans/s single tomograms..The last 8 groups, FA1, FA2, ..., FA30, are composites containing 1, 2, ..., 30 images at 92,000 A-scans/s.

Downloaded from SPIE Digital Library on 08 Jul 2011 to 129.97.72.149. Terms of Use: http://spiedl.org/terms

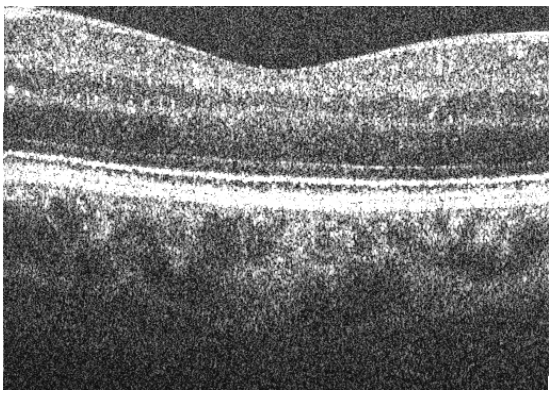

(a)

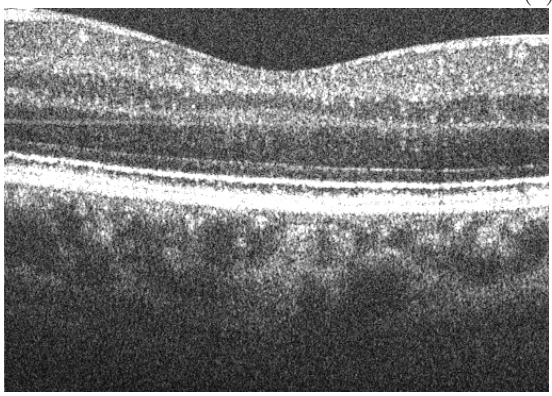

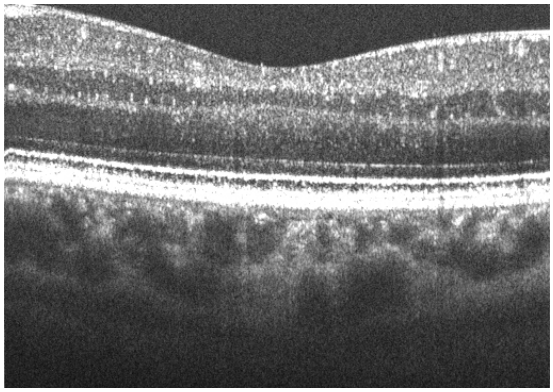

(b) (c)

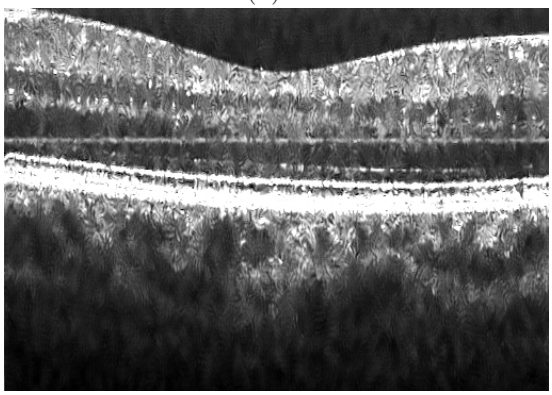

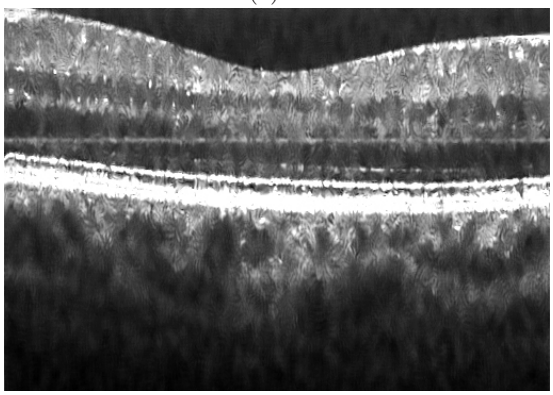

(d) (e)

Figure 2. Set 1, (a) single 92,000 A-scans/s tomogram, (b) composite of two 92,000 A-scans/s tomograms, (c) composite of ten 92,000 A-scans/s tomograms, (d) single 92,000 A-scans/s despeckled tomogram $\sigma = 26$, (e) single 92,000 A-scans/s despeckled tomogram $\sigma = 32$.

Downloaded from SPIE Digital Library on 08 Jul 2011 to 129.97.72.149. Terms of Use: http://spiedl.org/terms

The relationships between the SNR and CNR for the 47,000 A-scan/s and 92,000 A-scan/s images are shown in figure 1. This figure shows the results of an analysis of variance (ANOVA), which statistically tests whether the means of each category were equal.[3] Figure 1 shows that the CNR for the despeckled images is comparable to averaging two 47,000 A-scan/s tomograms or comparable to averaging up to twenty 92,000 A-scan/s tomograms. The lower portion of the figure shows that the SNR of the despeckled images is comparable to averaging between two and three 47,000 A-scan/s tomograms or comparable to averaging between ten and fifteen 92,000 A-scan/s tomograms. Table 1 contains the detailed metrics for 92,000 A-scan/s tomograms.

These results indicate that despeckling a single tomogram can obtain similar quality images as averaging multiple 47,000 and 92,000 A-scan/s tomograms. Data can be obtained around twice as fast as using the 47,000 system or about ten to fifteen times faster than using the 92,000 A-scan/s system. This is a major advantage of using despeckled tomograms.

The detailed ANOVA results are described below.

1. The despeckled images have a mean for the CNR and SNR that is statistically higher, with 95% confidence, than the corresponding means for a single slow image, single fast image, and a composite of two fast images.
2. The despeckled images have a mean for the CNR and SNR that is statistically lower, with 95% confidence, than the corresponding means for composites containing at least 10 slow images.
3. The despeckled images have a mean for the CNR and SNR that is within a 95% confidence interval for a composite of two slow images, a composite of five slow images, and composites containing between 5 and 30 fast images.
4. Composites containing at least 10 slow images have a mean for the CNR and SNR that is statistically higher, with 95% confidence, than composites containing less than 30 fast images.
5. A single slow image has a mean for the CNR and SNR that is statistically higher, with 95% confidence, than a single fast image.

The comparison of despeckled and composite tomograms can also be seen visually. Figure 2 illustrates the application of the despeckling algorithm compared to a single image captured at 92,000 A-scans/s and visual compares the result to two composite images. Figure 2b-e have less visible noise than figure 2a, the single tomogram. The composites containing 2 and 10 tomograms, figure 2b and c, are visually comparable to the despeckled tomograms figure 2d and figure 2e. The value for σ can be modified after the imaging session has been completed to find the value that produces the best image metrics. Figures 3 and 4 also provide additional comparisons.

4. CONCLUSION

Despeckling can reduce the imaging time by improving a single tomogram obtained using a high speed system. The quality obtained by despeckling a high speed tomogram is similar to that obtained using the average of two low speed tomograms (or similar to the average of ten to fifteen high speed tomograms). Despeckling can be much faster than averaging to obtain tomograms with similar image quality metrics.

If only averaging is used, the operator can image patients about 4 times faster using the despeckled 92,000 A-scans/s tomograms instead of composites obtained from single 47,000 A-scans/s. Statistical testing also demonstrates that a despeckled image from 1 tomogram is capable of providing similar CNR and SNR to 47,000 A-scans/s composites containing between 2 and 5 tomograms and 92,000 A-scans/s composites containing between 5 and 30 tomograms.

Ideally, despeckling can be combined with averaging to obtain very high quality tomograms that are visually appealing at a much higher rate than could be obtained using only averaging or using a much slower imaging system (which may be susceptible to motion artifacts).

The optimum value of σ can also be automatically determined (either during or after the image process) to generate a despeckled tomogram to maximize the image quality metrics. The image quality metrics can be extended to include subjective image quality metrics based on input from specialists.

Downloaded from SPIE Digital Library on 08 Jul 2011 to 129.97.72.149. Terms of Use: http://spiedl.org/terms

Table 1. Detailed SNR and CNR obtained from 8 retinal tomogram data sets captured at 92,000 A-scans/s.

			Absolute Value		Absolute Difference	
Set	Despeckle	# Samples	CNR	SNR	CNR	SNR
1	none	1	-0.96	17.99	0.00	0.00
1	none	2	-1.19	20.47	-0.23	2.47
1	none	5	-1.47	23.11	-0.52	5.12
1	$\sigma = 19$	1	-1.53	25.34	-0.58	7.35
1	$\sigma = 26$	1	-1.96	26.30	-1.00	8.30
1	$\sigma = 32$	1	-2.24	26.45	-1.28	8.45
2	none	1	-1.14	16.89	0.00	0.00
2	none	2	-1.34	19.21	-0.20	2.32
2	none	5	-1.52	21.63	-0.37	4.75
2	$\sigma = 19$	1	-1.52	23.09	-0.38	6.20
2	$\sigma = 26$	1	-1.72	24.12	-0.58	7.23
2	$\sigma = 32$	1	-1.89	24.26	-0.74	7.38
3	none	1	-1.03	17.57	0.00	0.00
3	none	2	-1.26	20.28	-0.23	2.71
3	none	5	-1.45	22.67	-0.42	5.10
3	none	10	-1.58	24.46	-0.55	6.89
4	none	1	-0.96	17.42	0.00	0.00
4	none	2	-1.13	19.78	-0.17	2.36
4	none	5	-1.34	22.15	-0.38	4.73
5	none	1	-0.91	17.65	0.00	0.00
5	none	2	-1.06	18.97	-0.15	1.32
5	none	5	-1.23	22.35	-0.33	4.70
5	none	10	-1.35	23.17	-0.45	5.52
5	$\sigma = 19$	1	-1.22	24.51	-0.31	6.86
5	$\sigma = 26$	1	-1.36	25.43	-0.45	7.78
5	$\sigma = 32$	1	-1.46	25.56	-0.55	7.92
6	none	1	-0.69	17.48	0.00	0.00
6	none	2	-0.82	19.90	-0.12	2.42
6	none	5	-0.93	22.16	-0.24	4.68
6	none	10	-0.95	22.60	-0.26	5.12
7	none	1	-1.11	17.65	0.00	0.00
7	none	2	-1.32	20.17	-0.21	2.52
7	none	5	-1.51	22.72	-0.40	5.07
7	none	10	-1.59	24.22	-0.49	6.57
7	none	15	-1.66	24.84	-0.55	7.19
8	none	1	-1.15	18.15	0.00	0.00
8	none	2	-1.41	20.84	-0.26	2.68
8	none	5	-1.62	23.51	-0.47	5.36
8	none	10	-1.76	25.10	-0.61	6.95
8	$\sigma = 19$	1	-1.57	25.91	-0.42	7.75
8	$\sigma = 26$	1	-1.79	26.66	-0.64	8.51
8	$\sigma = 32$	1	-1.93	26.77	-0.78	8.62

Downloaded from SPIE Digital Library on 08 Jul 2011 to 129.97.72.149. Terms of Use: http://spiedl.org/terms

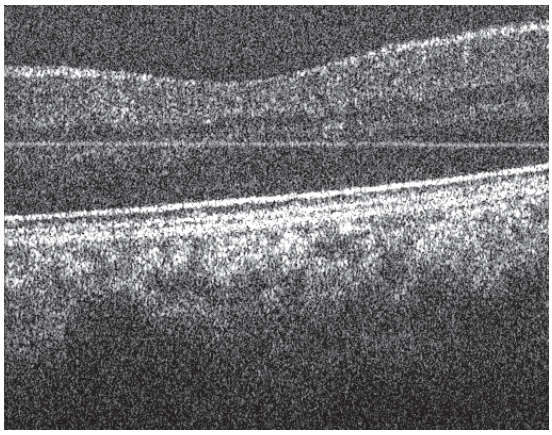

(a)

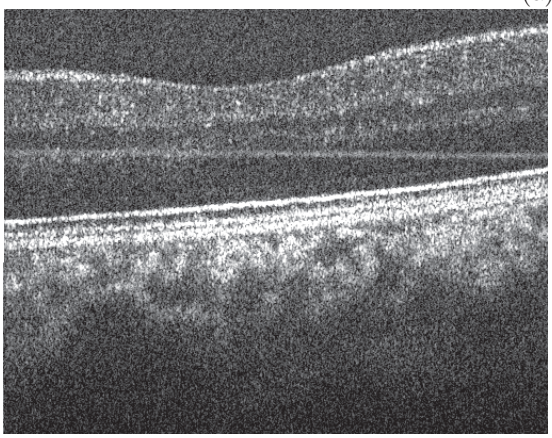

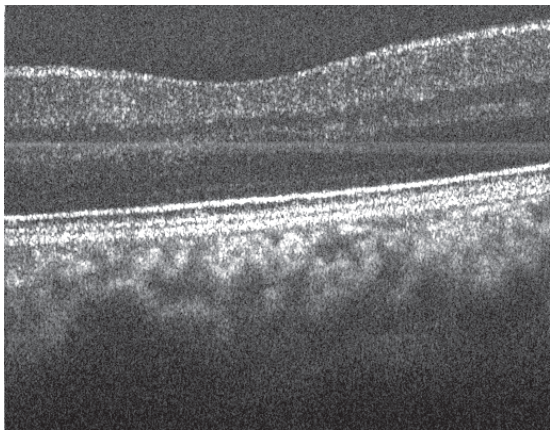

(b) (c)

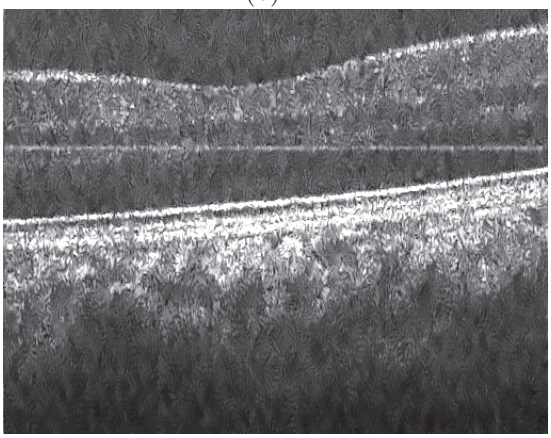

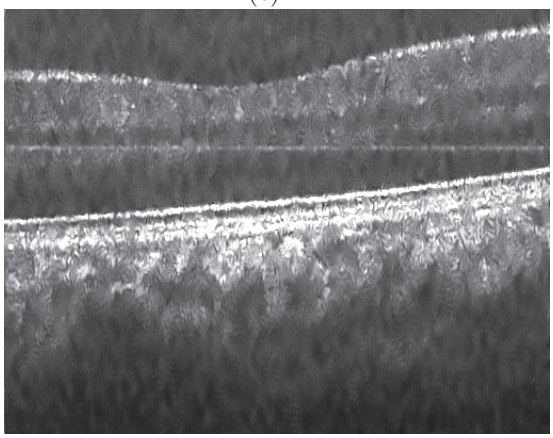

(d) (e)

Figure 3. Set 2, (a) single 92,000 A-scans/s tomogram, (b) composite of two 92,000 A-scans/s tomograms, (c) composite of five 92,000 A-scans/s tomograms, (d) single 92,000 A-scans/s despeckled tomogram $\sigma = 19$, (e) single 92,000 A-scans/s despeckled tomogram $\sigma = 26$.

Downloaded from SPIE Digital Library on 08 Jul 2011 to 129.97.72.149. Terms of Use: http://spiedl.org/terms

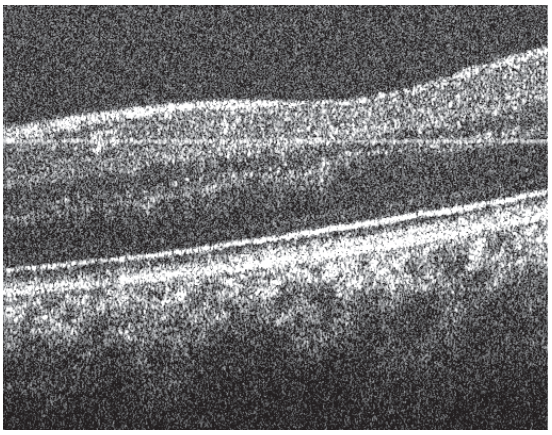

(a)

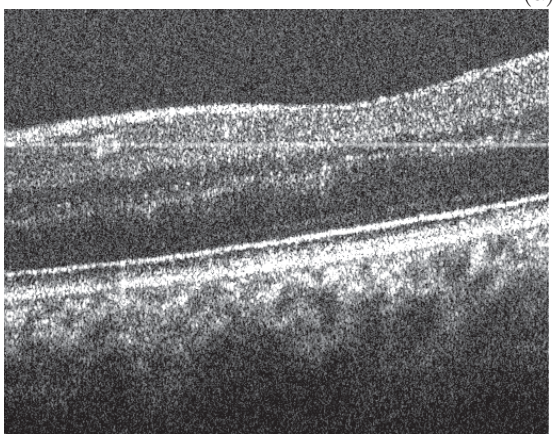

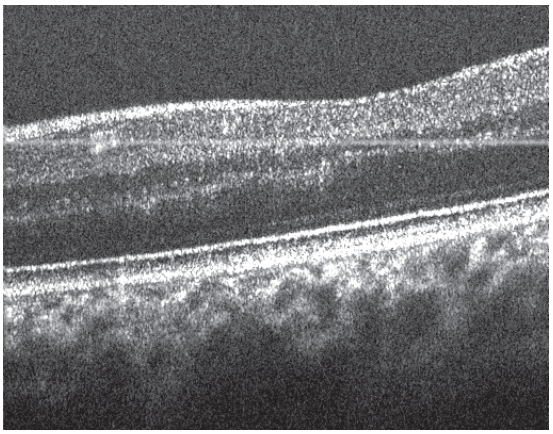

(b) (c)

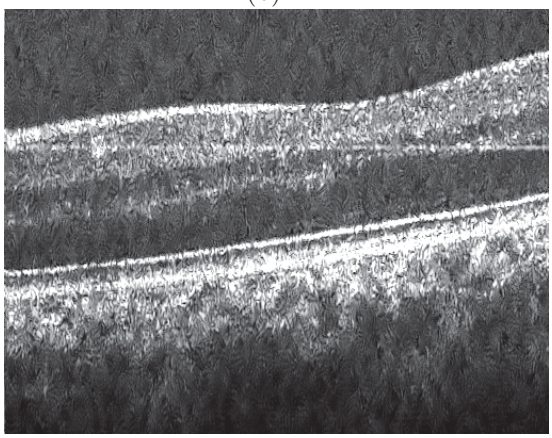

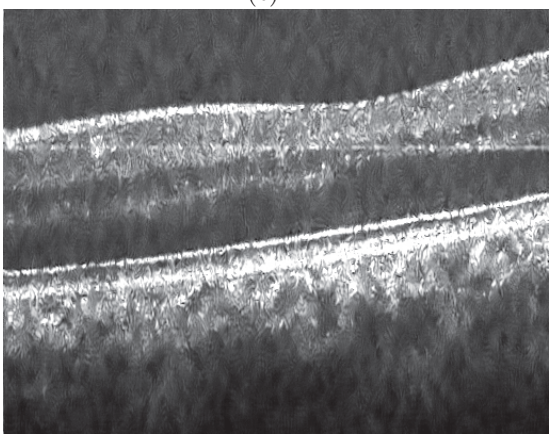

(d) (e)

Figure 4. Set 3, (a) single 92,000 A-scans/s tomogram, (b) composite of two 92,000 A-scans/s tomograms, (c) composite of five 92,000 A-scans/s tomograms, (d) single 92,000 A-scans/s despeckled tomogram $\sigma = 19$, (e) single 92,000 A-scans/s despeckled tomogram $\sigma = 26$.

Downloaded from SPIE Digital Library on 08 Jul 2011 to 129.97.72.149. Terms of Use: http://spiedl.org/terms

5. ACKNOWLEDGEMENTS

The authors would like to thank H. Van der Heide and K. Dvorski, from the Univ. of Waterloo Science shop for their assistance with electronic and mechanical designs, and P. Lee, J. Maram, G. Sorbara, T. Simpson and N. Hutchings for assistance with the retinal imaging. This project was funded in part by NSERC, CIHR and the University of Waterloo.

REFERENCES

[1] Puvanathasan, P., P. Forbes, Z. Ren, D. Malchow, S. Boyd, and K. Bizheva. "High-speed, High-Resolution Fourier-Domain Optical Coherence Tomography System for Retinal Imaging in the 1060 nm Wavelength Region." *Optics Letters*, 33(21), 2479-81 (2008).

[2] Wong, A., A. Mishra, D.A. Clausi, and K. Bizheva. "General Bayesian Estimation for Speckle Noise Reduction in Optical Coherence Tomography Retinal Imagery." *Optics Express*. 18(8), 8338-52 (2010).

[3] Hogg, R V and J Ledolter, *Applied Statistics for Engineers and Physical Scientists*, MacMillan, New York, N.Y., (1992).

[4] Lee, J. S., "Speckle suppression and analysis for synthetic aperture radar", *Opt. Eng.*, 25(5), 636-643 (1986).

[5] Frost, V. S., J. A. Stiles, K. S. Shanmugan, and J. C. Holtzman, "A model for radar images and its application to adaptive digital filtering for multiplicative noise", *IEEE Trans. Pattern Anal. Machine Intell.* 4,157-165 (1982).

[6] Kuan, D. T., A. A. Sawchuk, T. C. Strand, and P. Chavel, "Adaptive restoration of images with speckle", *IEEE Trans. Acoust., Speech, Signal Process.*, 35, 373-383 (1987).

[7] Loupas, T., W. Mcdicken, and P. Allen, "An adaptive weighted median filter for speckle suppression in medical ultrasound images", *IEEE Transactions on Circuits and Systems*, 36, 129135 (1989).

[8] Lopes, A. E., E. Nezry, R. Touzi, and H. Laur, "Structure Detection and Adaptive Speckle Filtering in SAR Images", *Int. J. Remote Sens.*, 14(9), 1735-1758 (1993).

[9] Yu, Y. and S. T. Acton, "Speckle reducing anisotropic diffusion", *IEEE Trans. Image Process.*, 11(11), 12601270 (2002).

[10] Krissian, K., C. Westin, R. Kikinis, and K. Vosburgh, "Oriented Speckle Reducing Anisotropic Diffusion", *IEEE Transactions on Image Processing*, 16(5), 1412-1424 (2007).

[11] A. Pizurica, W. Philips, I. Lemahieu, and M. Acheroy, "A versatile wavelet domain noise filtration technique for medical imaging", *IEEE Trans. Med. Imag.,*, 22(3), 323-331 (2003).

[12] H. Rabbani, M. Vafadust, P. Abolmaesumi, and S. Gazor, "Speckle Noise Reduction of Medical Ultrasound Images in Complex Wavelet Domain Using Mixture Priors," *IEEE Transactions Biomedical Engineering*, 55(9), 2152-2160 (2008).

Downloaded from SPIE Digital Library on 08 Jul 2011 to 129.97.72.149. Terms of Use: http://spiedl.org/terms